A stable Lagrange multiplier space for stiff interface conditions within the extended finite element method

Eric Béchet, Nicolas Moes, Barbara Wohlmuth

A stable Lagrange multiplier space for stiff interface conditions within the extended finite element method

Éric Béchet[1,*,†], Nicolas Moës[2] and Barbara Wohlmuth[3]

[1]*LTAS—Department of Aerospace and Mechanical Engineering, Université de Liège, Chemin des Chevreuils 1, 4000 Liège, Belgium*

[2]*Gem, Ecole Centrale de Nantes, Institut GEM, UMR CNRS 6183 1, rue de la Noë, 44321 Nantes, France*

[3]*Institute of Applied Analysis and Numerical Simulations (IANS), Universität Stuttgart, Pfaffenwaldring 57, 70529 Stuttgart, Germany*

This paper introduces a new algorithm to define a stable Lagrange multiplier space to impose stiff interface conditions within the context of the extended finite element method. In contrast to earlier approaches, we do not work with an interior penalty formulation as, e.g. for Nitsche techniques, but impose the constraints weakly in terms of Lagrange multipliers. Roughly speaking a stable and optimal discrete Lagrange multiplier space has to satisfy two criteria: a best approximation property and a uniform inf–sup condition. Owing to the fact that the interface does not match the edges of the mesh, the choice of a good discrete Lagrange multiplier space is not trivial. Here we propose a new algorithm for the local construction of the Lagrange multiplier space and show that a uniform inf–sup condition is satisfied. A counterexample is also presented, i.e. the inf–sup constant depends on the mesh-size and degenerates as it tends to zero. Numerical results in two-dimensional confirm the theoretical ones.

KEY WORDS: extended finite element method; stiff boundary condition; Lagrange multiplier space

1. INTRODUCTION

The extended finite element method (X-FEM) is an extension of the finite element method to handle physical domains whose boundaries are not necessarily exactly meshed or to deal with physical surfaces crossing elements. The physical surfaces are handled inside the elements using enrichment functions that model the appropriate discontinuity. This enrichment is introduced inside the mesh using the so-called partition of unity technique [1, 2]. The X-FEM was first introduced to model two-dimensional cracks in [3, 4]. It was then extended to 3D in [5, 6]. The modeling of

*Correspondence to: Éric Béchet, LTAS—Department of Aerospace and Mechanical Engineering, Université de Liège, Chemin des Chevreuils 1, 4000 Liège, Belgium.

†E-mail: eric.bechet@ulg.ac.be

tangential discontinuities can be found in [7]. The modeling of voids was considered in [8] and of material interfaces in [9, 10].

Imposing Neumann or traction-free conditions on crack faces or along the boundary of a hole does not require any special effort with the X-FEM. Just like with classical displacement-based finite elements, no additional term on the traction-free surface enters, and a straightforward integration takes place if Neumann boundary conditions are present. The situation is drastically different in the case of stiff conditions, e.g. as by imposing Dirichlet boundary conditions or contact on the faces of a crack. The imposition of stiff constraints may also be needed to glue together two different materials or in the case of phase transformation and contact problems. The major issue is how to ensure that stiff constraints are correctly imposed and also to ensure that the corresponding fluxes are accurate and non-oscillating. In many applications, the fluxes are quite important, e.g. the front in phase transformation problems or the growth of a crack in contact problems is governed by fluxes.

In order to impose stiff boundary/interface conditions along an interface that is not conforming with the mesh, two major approaches can be found in the literature: variants of the Nitsche approach and the use of Lagrange multipliers. The latter is the focus of this paper, but we first recall the main works related to the Nitsche method.

In the seventies, Nitsche [11] considered Dirichlet boundary conditions over a non-conforming boundary and introduced a one-field variational formulation taking into account the inner equilibrium as well as the Dirichlet boundary condition. The formulation involves a parameter that must be chosen with care in order to get a stable formulation. Note that the choice of this parameter was discussed in the mesh-free framework in [12]. The Nitsche variational formulation was extended to model material interfaces in [13] so that the different material phases are 'glued' together with a Nitsche-type formulation. Although attractive, Nitsche's approach has the drawback to be difficult to extend to other stiff boundary conditions as contact, though this kind of formulation has been used recently in contact problems with a kind of penalty stabilization in [14]. In addition, the use of a non-linear bulk material law is not straightforward. The parameter in Nitsche's method has to be determined and that parameter depends also on the physical problem. Efforts were done recently in order to determine automatically this parameter using bubble stabilization [15, 16]. In [17], Stenberg shows that stabilization in mixed finite element methods is closely related to Nitsche's approach.

In this paper, we consider instead a Lagrange multiplier approach. More precisely, we introduce a Lagrange multiplier space, and the fluxes across the interface or on the boundary are used as additional unknowns. The original variable is referred to as primal and the new one as dual variable. In terms of the pair of primal and dual variables all types of constraints can be easily handled, e.g. stiff Robin-type conditions. Lagrange multipliers were considered for the first time within the concept of X-FEM in [18]. In [19], the authors illustrate through numerical experiments that a naive choice for the Lagrange multiplier space, i.e. a piecewise linear ansatz space on the interface with a degree of freedom at each node obtained by cutting the interface with the edges of the two-dimensional mesh of the primal variable, yields oscillatory multipliers on the boundary. As pointed out in [15], these oscillations were also noticed by Simone [20] in the context of stiff cohesive law imposed on the faces of a crack. This oscillatory effect is referred to as boundary locking. From the mathematical point of view, these oscillations result from a non-uniform but mesh-dependent inf–sup condition. Roughly speaking this means that the Lagrange multiplier space is locally too rich, and as a consequence the constant in the inf–sup condition tends to zero if the mesh-size tends to zero.

In order to improve the approach, a first effort was done in [21] where a reduced Lagrange multiplier space has been proposed. Although the algorithm to define the Lagrange multiplier space passes a numerical inf–sup test, it is quite complex. Numerically, the Chapelle–Bathe test is used quite often [22, 23] to verify the inf–sup condition. This test reduces to the computation of eigenvalues for a sequence of meshes with increasing density. This test was already used in [21]. A second algorithm was then proposed in [24], and it is currently extended for large sliding [25]. The strategy used to build the Lagrange multiplier space in the second algorithm is quite easy to grasp. We consider the nodes on each side of the interface. These nodes are tied together across the interface by cut edges. As a subset of these cut edges, we define the set of vital edges as the minimum set of edges able to connect the nodes on each side of the interface. These vital edges and only these will hold a Lagrange multiplier degree of freedom. This second algorithm showed slight improvement in terms of accuracy compared with the first one. The major issue in implementing the second algorithm is that finding the vital edges requires to solve a global problem. Although both approaches perform numerically rather well and no oscillations can be observed, no theoretical analysis of the stability exists. An alternative Lagrange multiplier-based strategy has also been studied recently in [26]. Finally, a stabilization of the Lagrange multipliers based on the Barbosa and Hugues approach has been introduced in [27].

In the present paper, we introduce a new algorithm allowing a local construction of the Lagrange multiplier space while improving the accuracy of the computed fields. The originality of this approach with regard to [21] lies in the use of the trace of primary shape functions defined on the domain, and a simplified procedure to define the mesh on the interface. The proper design of the Lagrange multiplier space is guided by the inf–sup condition [28–30]. Moreover, we show that the newly constructed Lagrange multiplier space satisfies, in contrast to the naive approach, a uniform inf–sup condition.

2. MODEL PROBLEM

We are concerned in this paper by interfaces over which the mechanical stiffness is high. Dirichlet conditions are the limit for infinite stiffness, whereas Neumann-type conditions may be seen as the limit for a zero stiffness. In the case of a non-linear interface law such as, e.g. contact or a cohesive law, a sequence of linear systems has to be solved to find the solution of the non-linear problem. Each linear system may involve high stiffness over the interface.

We consider a polygonal domain $\Omega \subset \mathbb{R}^2$, which is possibly decomposed by a non-empty interface Γ into two subdomains Ω_i, $i=1,2$, of regular shape. In that case, we assume $\bar{\Gamma}=\partial\Omega_1 \cap \partial\Omega_2$, and we decompose $\partial\Omega$ into two open parts Γ_D and Γ_N such that $\Gamma_D \cap \Gamma_N = \emptyset$. Otherwise, we split $\partial\Omega$ into three disjoint open parts Γ_D, Γ_N and $\Gamma \neq \emptyset$ and set formally $\Omega_1 := \Omega$, $\Omega_2 := \emptyset$. On Γ_D homogeneous Dirichlet boundary conditions are given, and on Γ_N we impose inhomogeneous Neumann boundary conditions t_N. Stiff interface/boundary conditions in terms of a given u_D and a stiffness parameter $k>0$ are considered on Γ. Associated with the Laplace operator on Ω and a given volume force f, the weak one-field variational problem is defined by: Find $u \in \mathscr{U} := \{v \in H^1(\Omega_1) \times H^1(\Omega_2), v_{|\Gamma_D} = 0\}$ such that for all $v \in \mathscr{U}$

$$\int_\Omega \nabla u \cdot \nabla v \, d\Omega + \int_\Gamma k[u][v] \, d\Gamma = \int_\Omega f v \, d\Omega + \int_{\Gamma_N} t_N v \, d\Gamma_N + \int_\Gamma k u_D [v] \, d\Gamma \tag{1}$$

The interface/boundary integral on Γ is the variational form of the stiff spring-type condition

$$\nabla_n u = -k([u] - u_{\mathrm{D}})$$

where $\nabla_n u$ is the flux on Γ outward to Ω_1 and $[u] := u_{|\Omega_1} - u_{|\Omega_2}$ and $u_{|\Omega_2} := 0$ if Ω_2 is the empty set. We note that under the assumption that Γ_{D} is a non-empty open set and $k > 0$, the variational problem defined by (1) has a unique solution.

However for large values of k, the discretized variational principle has very poor performance and locking effects can be observed. To overcome this difficulty, a two-field variational formulation can be considered. Introducing $\lambda := -\nabla_n u$ as additional unknown variable, we obtain the following saddle-point problem: Find $(u, \lambda) \in \mathscr{U} \times \mathscr{L}$ such that

$$\int_\Omega \nabla u \cdot \nabla v \, \mathrm{d}\Omega + \langle \lambda, [v] \rangle_\Gamma = \int_\Omega f v \, \mathrm{d}\Omega + \int_{\Gamma_{\mathrm{N}}} t_{\mathrm{N}} v \, \mathrm{d}\Gamma_{\mathrm{N}} \quad \forall v \in \mathscr{U} \tag{2}$$

$$\langle \mu, [u] \rangle_\Gamma - \frac{1}{k} (\mu, \lambda)_{-1/2;\Gamma} = \langle \mu, u_{\mathrm{D}} \rangle_\Gamma \quad \forall \mu \in \mathscr{L} \tag{3}$$

where $\mathscr{L} := (H^{1/2}(\Gamma))'$ is the dual space of the trace space of $\mathscr{U}$ restricted to Γ. Here we assume for simplicity that $\bar{\Gamma} \cap \bar{\Gamma}_{\mathrm{D}} = \emptyset$. Otherwise, we have to work with the dual space of a suitable subspace of $H^{1/2}(\Gamma)$. We remark that in the general situation a careful distinction between $H^{1/2}(\Gamma)$ and $H_{00}^{1/2}(\Gamma)$ is required. By $\langle \cdot, \cdot \rangle_\Gamma$ we denote the duality pairing between $\mathscr{L}$ and the trace of $\mathscr{U}$, and by $(\cdot, \cdot)_{-1/2;\Gamma}$ the natural scalar product on $\mathscr{L}$, which can be identified with the L^2-scalar-product in the discrete setting.

Note that (3) stays well defined in the limit of k becoming infinite (Dirichlet conditions or perfect bonding along an interface). Existence and uniqueness of a weak solution (u, λ) is guaranteed within the abstract framework of saddle-point problems, see, e.g. [30].

The discretization of the saddle-point problem (2)–(3) involves a pair of finite element spaces $\mathscr{U}^h \subset \mathscr{U}$ and $\mathscr{L}^h \subset \mathscr{L}$ leading to the discrete formulation: Find $(u^h, \lambda^h) \in \mathscr{U}^h \times \mathscr{L}^h$ such that

$$\int_\Omega \nabla u^h \cdot \nabla v^h \, \mathrm{d}\Omega + \langle \lambda^h, [v^h] \rangle_\Gamma = \int_\Omega f v^h \, \mathrm{d}\Omega + \int_{\Gamma_{\mathrm{N}}} t_{\mathrm{N}} v^h \, \mathrm{d}\Gamma_{\mathrm{N}} \quad \forall v^h \in \mathscr{U}^h \tag{4}$$

$$\langle \mu^h, [u^h] \rangle_\Gamma - \frac{1}{k} (\mu^h, \lambda^h)_{-1/2;\Gamma} = \langle \mu^h, u_{\mathrm{D}} \rangle_\Gamma \quad \forall \mu^h \in \mathscr{L}^h \tag{5}$$

Here, we restrict ourselves to low-order conforming finite elements for $\mathscr{U}^h$ associated with a family of shape regular triangulations $\mathscr{T}_h$. We note that in general $\mathscr{T}_h$ is not adapted to Γ and thus Ω_1 cannot be written as union of elements in $\mathscr{T}_h$. More precisely, as standard within the X-FEM approach $\mathscr{U}^h := \mathscr{U}_1^h \times \mathscr{U}_2^h$, where $\mathscr{U}_i^h$ is the conforming finite element space with respect to the mesh $\mathscr{T}_h$ on Ω restricted to Ω_i. In the numerical implementation it is sufficient to double the degrees of freedom at vertices which belong to an element which is cut by Γ, see, e.g. [4].

The choice of the finite element spaces $\mathscr{U}^h$ and $\mathscr{L}^h$ has to satisfy a uniform inf–sup condition [23, 30] with respect to suitable norms. In the discrete setting quite often it is of interest to work with a weighted pair of L^2-norms instead of the $H^{1/2}(\Gamma)$ and $H^{-1/2}(\Gamma)$ duality pair. To do so,

we consider the mesh-dependent L^2-norms

$$\begin{aligned} \|\mu^h\|^2_{-1/2;\Gamma_h} &:= \sum_{e\in\mathscr{E}_h} h_e \|\mu^h\|^2_{0;e} \\ \|v^h\|^2_{1/2;\Gamma_h} &:= \sum_{e\in\mathscr{E}_h} \frac{1}{h_e} \|v^h\|^2_{0;e} \end{aligned} \tag{6}$$

where $\mathscr{E}_h$ stands for the set of elements of the one-dimensional mesh on Γ which defines the Lagrange multiplier space and h_e denotes the length of e. In our case the uniform inf–sup condition requires that there exists a positive constant α independent of the mesh-size h such that

$$\inf_{\mu^h\in\mathscr{L}^h} \sup_{v^h\in\mathscr{U}^h} \frac{\int_\Gamma \mu^h [v^h]\,\mathrm{d}\Gamma}{\|\mu^h\|_{-1/2;\Gamma_h}\|v^h\|_{1;\Omega}} \geqslant \alpha > 0 \tag{7}$$

where $\|\cdot\|_{1;\Omega}$ stands for the broken H^1-norm, i.e. $\|\cdot\|^2_{1;\Omega} := \|\cdot\|^2_{1;\Omega_1} + \|\cdot\|^2_{1;\Omega_2}$.

For many practical situations, it is quite difficult to show the existence of such a mesh-independent inf–sup constant α. In that case, the numerical inf–sup test [22] may be used. As mentioned before, this test reduces to the computation of eigenvalues for a sequence of meshes of increasing density.

Let U_h and Λ_h be the vectors of the potential and the Lagrange multiplier, respectively. Then, the algebraic form of the variational problem (4)–(5) is given by

$$\begin{pmatrix} A_h & B_h^{\mathrm{T}} \\ B_h & -\dfrac{1}{k} M_h \end{pmatrix} \begin{pmatrix} U_h \\ L_h \end{pmatrix} = \begin{pmatrix} F_h \\ D_h \end{pmatrix} \tag{8}$$

where A_h is the stiffness matrix associated with the Laplace operator and M_h corresponds to a symmetric mass matrix on Γ. The stability and well-posedness of the system depends highly on the properties of the coupling matrix B_h. Let us assume at the moment for simplicity that $\Gamma_{\mathrm{D}} \cap \partial\Omega_i$, $i = 1, 2$, is non-empty then the stiffness matrix A_h is symmetric and positive definite and $V_h^{\mathrm{T}} A_h V_h$ is equivalent to $\|v^h\|^2_{1;\Omega}$, where V_h is the algebraic representation of $v^h \in \mathscr{U}^h$. Furthermore, if the mesh on Γ is uniform, i.e. there exist constants such that $\hat{c}h \leqslant h_e \leqslant \hat{C}h$ for all $e \in \mathscr{E}_h$, then $h\Upsilon_h^{\mathrm{T}} M_h \Upsilon_h$ is equivalent to $\|v^h\|^2_{-1/2;\Gamma_h}$, where Υ_h is the algebraic representation of $v^h \in \mathscr{L}^h$. Using these norm equivalences, we can rewrite (7) in an equivalent algebraic form as

$$\inf_{\Upsilon_h\in\mathbb{R}^{m_h}} \sup_{V_h\in\mathbb{R}^{n_h}} \frac{(\Upsilon_h^{\mathrm{T}} B_h V_h)^2}{h\Upsilon_h^{\mathrm{T}} M_h \Upsilon_h V_h^{\mathrm{T}} A_h V_h} \geqslant \hat{\alpha}^2 > 0 \tag{9}$$

where m_h and n_h stand for the dimensions of $\mathscr{L}^h$ and $\mathscr{U}^h$, respectively, and $\hat{\alpha}$ and α are equivalent. More precisely, a mesh-size-independent α in (7) exists if and only if a mesh-size-independent $\hat{\alpha}$ in (9) exists.

From (9), the numerical inf–sup test can be motivated. In practice, the inf–sup test reduces to the solution of a eigenvalue problem using a sequence of three to four meshes $\mathscr{T}_h$, $h \in \{h_i, i = 1, \ldots, N\}$, with decreasing mesh-size, see [22]. Here for convenience of the reader, we will recall two variants.

The first variant is given by the following eigenvalue problem:

$$\frac{1}{h}(B_h^{\mathrm{T}} M_h^{-1} B_h) V_h = \beta_h A_h V_h \tag{10}$$

We denote the first non-zero eigenvalue by $\beta_{h;\min}$, then the value of α is approximated by $\min_{h_i, i=1,\ldots,N} \sqrt{\beta_{h;\min}}$.

The second variant is given by the following eigenvalue problem:

$$\frac{1}{h}(B_h A_h^{-1} B_h^{\mathrm{T}}) \Upsilon_h = \beta_h M_h \Upsilon_h \tag{11}$$

The first non-zero eigenvalue of (10) is the same as the first non-zero eigenvalue of (11).

We recall that a necessary condition for the existence of an inf–sup constant is that $m_h \leqslant n_h$ and that B_h has full rank. Then for each $\Upsilon_h \in \mathbb{R}^{m_h}$, we can find a $V_h \in \mathbb{R}^{n_h}$ such that $\Upsilon_h = M_h^{-1} B_h V_h$ and

$$\frac{(\Upsilon_h^{\mathrm{T}} B_h V_h)^2}{h \Upsilon_h^{\mathrm{T}} M_h \Upsilon_h V_h^{\mathrm{T}} A_h V_h} = \frac{V_h^{\mathrm{T}} B_h^{\mathrm{T}} M_h^{-1} B_h V_h}{h V_h^{\mathrm{T}} A_h V_h}$$

These considerations motivate the first variant of the numerical inf–sup test. The second variant is obtained by setting $V_h = A_h^{-1} B_h^{\mathrm{T}} \Upsilon_h$ and thus

$$\frac{(\Upsilon_h^{\mathrm{T}} B_h V_h)^2}{h \Upsilon_h^{\mathrm{T}} M_h \Upsilon_h V_h^{\mathrm{T}} A_h V_h} = \frac{\Upsilon_h^{\mathrm{T}} B_h A_h^{-1} B_h^{\mathrm{T}} \Upsilon_h}{h \Upsilon_h^{\mathrm{T}} M_h \Upsilon_h}$$

Remark 2.1
If the inf–sup condition (7) is uniformly satisfied, i.e. with a constant independently of the mesh-size, and the discrete Lagrange multiplier space satisfies the best approximation property

$$\inf_{\mu^h \in \mathscr{L}^h} \|\lambda - \mu^h\|_{-1/2;\Gamma_h} = \mathcal{O}(h)$$

for $\lambda \in H^{1/2}(\Gamma)$, then the two-field approach (4)–(5) yields stable numerical results, and optimality of the discretization error follows from the saddle-point theory [30]. We note that for the best approximation property of $\mathscr{L}^h$ it is sufficient that the basis function of $\mathscr{L}^h$ have a local support and that constants can be reproduced by the Lagrange multiplier space.

3. COUNTEREXAMPLE

The following example shows that a naive approach to define the Lagrange multiplier space $\mathscr{L}^h$ fails. For simplicity, we assume that the unit square $\Omega := (0,1)^2$ is decomposed by the interface $\Gamma := \{y = 0.5\}$ into two rectangles. The uniform mesh on Ω is given by $2(n-1)^2$, $n := 2k$ triangles, where $h := 1/(n-1)$, see Figure 1.

We note that typically finite elements spaces are given by a mesh and a basis type. Here, we use standard hat functions, i.e. piecewise linear and continuous functions, as basis. In a first setting, the nodes of the one-dimensional mesh are given by the intersection of the interface Γ with the edges of the triangulation on Ω, see Figure 1. Thus, we obtain a uniform mesh with $2n-1$ nodes and

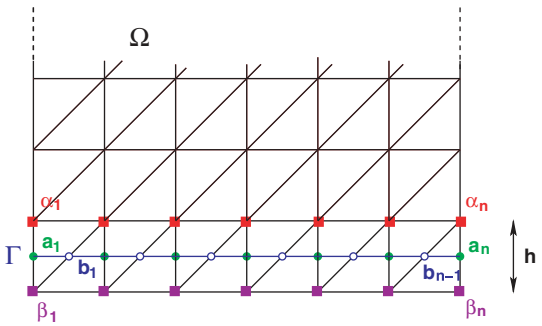

Figure 1. Interface and triangulation, $n=8$.

edges of length $h/2$. To show that this naive approach does not yield a uniform inf–sup condition, we consider two special cases.

In our first example, the coefficients of $\mu^h \in \mathscr{L}^h$ with respect to the nodal basis are given by $a_l = 1$, $l = 1, \ldots, n$, and $b_l = -1$, $l = 1, \ldots, n-1$. Then, it is easy to see that the L^2-norm of μ^h can be bounded from above and below by positive constants independent of h. Moreover, the weighted L^2-norm of μ^h is uniformly equivalent to $\sqrt{h}$, i.e.

$$\hat{c}\sqrt{h} \leqslant \|\mu^h\|_{-1/2;\Gamma_h} \leqslant \hat{C}\sqrt{h} \tag{12}$$

Because of the position of the interface and the locality of the support only the coefficients $\alpha_l := \alpha_l^1 - \alpha_l^2$ and $\beta_l := \beta_l^1 - \beta_l^2$, $1 \leqslant l \leqslant n$, of $v^h \in \mathscr{W}^h$ enter into the computation of $\int_\Gamma [v^h]\mu^h \, \mathrm{d}\Gamma$. Here, α_l^i, β_l^i, $1 \leqslant i \leqslant 2$, are the coefficients in the nodal basis of $v^h \in \mathscr{W}^h$ restricted to Ω_i. The values of v^h at the nodes marked by a filled bullet in Figure 1 are given by $0.5(\alpha_l + \beta_l)$ and at the nodes marked by an empty bullet by $0.5(\beta_l + \alpha_{l+1})$. Then, it is easy to see that

$$\begin{aligned}
\int_\Gamma \mu^h [v^h] \, \mathrm{d}\Gamma &= \sum_{l=1}^{n-1} \frac{h}{24} ((\alpha_l + \beta_l - (\beta_l + \alpha_{l+1})) + (\alpha_{l+1} + \beta_{l+1} - (\beta_l + \alpha_{l+1}))) \\
&= \sum_{l=1}^{n-1} \frac{h}{24} (\alpha_l - \alpha_{l+1} + \beta_{l+1} - \beta_l) = \frac{h}{24} (\alpha_1 - \beta_1 + \beta_n - \alpha_n) \\
&\leqslant Ch(|\alpha_1 - \beta_1| + |\alpha_n - \beta_n|) \\
&\leqslant Ch(|\alpha_1^1 - \beta_1^1| + |\alpha_n^1 - \beta_n^1| + |\alpha_1^2 - \beta_1^2| + |\alpha_n^2 - \beta_n^2|) \\
&\leqslant Ch(\|v^h\|_{1;\Omega_1} + \|v^h\|_{1;\Omega_2}) \leqslant Ch\|v^h\|_{1;\Omega}
\end{aligned}$$

Here, we have used a standard norm equivalence for piecewise linear elements, i.e. for all $w \in P_1(T)$ we have that $\sum_{i,j=1}^3 (w(p_i) - w(p_j))^2$ is equivalent to the squared $H^1(T)$-seminorm $|w|_{1;T}^2$, where p_i, $1 \leqslant i \leqslant 3$, are the three nodes of the triangle T. The previous inequality shows that

$$\sup_{v^h \in \mathscr{W}^h} \frac{\int_\Gamma \mu^h [v^h] \, \mathrm{d}\Gamma}{\|v^h\|_{1;\Omega}} \leqslant Ch \leqslant C\sqrt{h}\|\mu^h\|_{-1/2;\Gamma_h}$$

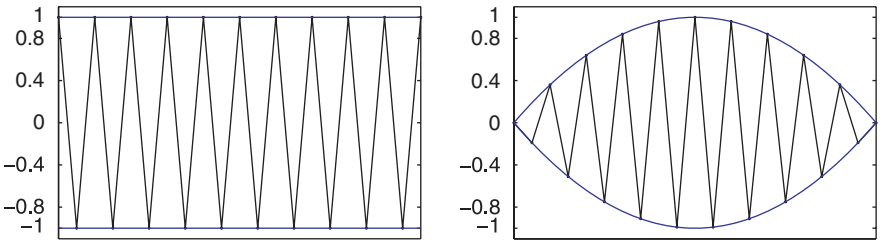

Figure 2. Structure of the first counterexample (left) and the second one (right).

and as a result there is no uniform inf–sup estimate. This simple counterexample shows that a naive choice for the degrees of freedom for $\mathscr{L}^h$ does not yield optimal *a priori* estimates. From a non-uniform inf–sup estimate, poor numerical results can be expected and oscillations in the Lagrange multiplier can be observed. This effect is similar to the well-known checkerboard modes for the Stokes system.

The second example shows that the best constant we can find in the inf–sup estimate is not of $\mathcal{O}(h^{1/2})$ as it might be expected from the first example. We specify the coefficients of $\mu^h \in \mathscr{L}^h$ with respect to the nodal basis by $a_l = (l-1)(n-l)$, $l = 1, \ldots, n$, and $b_l = -(l-0.5)(n-l-0.5)$, $l = 1, \ldots, n-1$, see Figure 2. Then, it is trivial to see that $a_1 = a_n = 0$ and thus $\sum_{l=1}^{n-1} a_l \gamma_l = \sum_{l=1}^{n-1} a_{l+1}\gamma_{l+1}$ and moreover, we find for $l = 1, \ldots, n-1$

$$2b_l + a_l + a_{l+1} = -\tfrac{1}{2}, \quad a_{l+1} - a_l = n - 2l \tag{13}$$

The $\|\cdot\|^2_{-1/2;\Gamma_h}$-norm of μ^h is equivalent to

$$\|\mu^h\|^2_{-1/2;\Gamma_h} \equiv h^2 \sum_{l=1}^{n-1} (a_l^2 + b_l^2) \equiv h^2 \sum_{l=1}^{n-1} l^4 \equiv h^2 \mathcal{O}(n^5) \equiv \mathcal{O}(n^3)$$

Figure 2 shows the structure of the two counterexamples. In both cases the coefficients are oscillating, the absolute values of the coefficients are constant in the first example, and in the second they follow a quadratic function.

Decomposing Γ into $(n-1)$-subintervals of length h and using the fact that the values of $[v^h]$, $v^h \in \mathscr{W}^h$ at the intersection nodes are given by $\frac{1}{2}(\alpha_l + \beta_l)$, $\frac{1}{2}(\alpha_{l+1} + \beta_l)$, $\frac{1}{2}(\alpha_{l+1} + \beta_{l+1})$, we obtain for the coupling between v^h and μ^h

$$\begin{aligned}
\int_\Gamma \mu^h [v^h] \, \mathrm{d}\Gamma &= \frac{h}{24} \sum_{l=1}^{n-1} ((\alpha_l + \beta_l)(2a_l + b_l) + (\beta_l + \alpha_{l+1})(2b_l + a_l + 2b_l + a_{l+1}) \\
&\quad + (\alpha_{l+1} + \beta_{l+1})(2a_{l+1} + b_l)) \\
&= \frac{h}{24} \sum_{l=1}^{n-1} \left(\frac{1}{2}(2b_l + a_l + a_{l+1})(\alpha_l + 5\beta_l + 5\alpha_{l+1} + \beta_{l+1}) \right. \\
&\quad \left. + \left(\frac{1}{2}(a_l - a_{l+1}) + a_l \right)(\alpha_l + \beta_l) - (a_l + a_{l+1})(\alpha_{l+1} + \beta_l) \right)
\end{aligned}$$

$$+\left(-\frac{1}{2}(a_l-a_{l+1})+a_{l+1}\right)(\alpha_{l+1}+\beta_{l+1})\Bigg)$$

$$=\frac{h}{24}\sum_{l=1}^{n-1}\Bigg(-\frac{1}{4}(\alpha_l+5\beta_l+5\alpha_{l+1}+\beta_{l+1})$$

$$+\frac{1}{2}(n-2l)((\alpha_{l+1}-\alpha_l)+(\beta_{l+1}-\beta_l)+(\alpha_{l+1}-\beta_l))\Bigg)$$

Applying Cauchy–Schwarz and using $\sum_{l=1}^{n-1}1=\mathcal{O}(n)$, $\sum_{l=1}^{n-1}(n-2l)^2=\mathcal{O}(n^3)$, we find in terms of (13)

$$\left(\int_\Gamma \mu^h[v^h]\,\mathrm{d}\Gamma\right)^2 \leqslant C\frac{1}{n}\sum_{l=1}^{n}(\alpha_l^2+\beta_l^2)+Cn\sum_{l=1}^{n-1}(\alpha_{l+1}-\alpha_l)^2$$

$$+(\beta_{l+1}-\beta_l)^2+(\alpha_{l+1}-\beta_l)^2$$

$$\leqslant Cn(\|v^h\|_{0;\Omega}^2+|v^h|_{1;\Omega}^2)\leqslant Ch^2\|v^h\|_{1;\Omega}^2\|\mu^h\|_{-1/2;\Gamma_h}^2$$

These two examples illustrate why a naive choice of the Lagrange multiplier space fails, and that there exists no mesh-independent constant such that (7) holds. We refer to [21] in which numerical tests are based on such a situation. In the following lemma, we show how the inf–sup constant in (7) depends on the mesh-size.

Lemma 3.1
There exists a constant independent of h such that for all $\mu^h\in\mathscr{L}^h$

$$\sup_{v^h\in\mathscr{U}^h}\frac{\int_\Gamma \mu^h[v^h]\,\mathrm{d}\Gamma}{\|v^h\|_{1;\Omega}}\geqslant ch\|\mu^h\|_{-1/2;\Gamma_h}$$

Proof
It is easy to see that for $\mu^h\in\mathscr{L}^h$, the weighted L^2-norm $\|\mu^h\|_{\sqrt{h};\Gamma}^2$ is equivalent to $h^2\sum_{i=1}^n(a_i^2+b_i^2)$, where a_i and b_i are the coefficients of μ^h and $b_n:=0$. Now, we set the coefficient α_1^1 of $v_{\mu^h}^h\in\mathscr{U}^h$ to be zero and require for β_1^1 and α_i^1,β_i^1, $i=2,\ldots,n$, that $\alpha_i^1+\beta_i^1=2a_i$, $1\leqslant i\leqslant n$, and that $\alpha_{i+1}^1+\beta_i^1=2b_i$, $1\leqslant i\leqslant n-1$. All other coefficients of $v_{\mu^h}^h$ are set to be zero and thus $\alpha_i=\alpha_i^1$, $\beta_i=\beta_i^1$. We note that these conditions define $v_{\mu^h}^h\in\mathscr{U}^h$ uniquely. Observing that for each element in $\mathscr{U}^h$, the trace of its jump on Γ is in $\mathscr{L}^h$, it is easy to see that $[v_{\mu^h}^h]|_\Gamma=\mu^h$ and thus $h\int_\Gamma\mu^h[v^h]_{\mu^h}\,\mathrm{d}\Gamma=\|\mu^h\|_{-1/2,\Gamma_h}^2$. Then an inverse estimate gives that $\|v_{\mu^h}^h\|_{1;\Omega}^2=\|v_{\mu^h}^h\|_{1;\Omega_1}^2$ is equivalent to $\sum_{i=1}^n(\alpha_i^2+\beta_i^2)$ and thus

$$\sup_{v^h\in\mathscr{U}^h}\frac{\int_\Gamma \mu^h[v^h]\,\mathrm{d}\Gamma}{\|v^h\|_{1;\Omega}}\geqslant ch\frac{\sum_{i=1}^n(a_i^2+b_i^2)}{(\sum_{i=1}^n(\alpha_i^2+\beta_i^2))^{0.5}}\geqslant c\frac{(\sum_{i=1}^n(a_i^2+b_i^2))^{0.5}}{(\sum_{i=1}^n(\alpha_i^2+\beta_i^2))^{0.5}}\|\mu^h\|_{\sqrt{h};\Gamma}$$

Observing that the two sets of coefficients are related by the lower tridiagonal matrix C of size $(2n-1)\times(2n-1)$

$$Cw := \begin{pmatrix} 1 & & & & & \\ 1 & 1 & & & & \\ & 1 & 1 & & & \\ & & 1 & 1 & & \\ & & & 1 & 1 & \\ & & & & \ddots & \ddots \end{pmatrix} \begin{pmatrix} \beta_1 \\ \alpha_2 \\ \beta_2 \\ \vdots \\ \alpha_n \\ \beta_n \end{pmatrix} = 2 \begin{pmatrix} a_1 \\ b_1 \\ a_2 \\ \vdots \\ b_{n-1} \\ a_n \end{pmatrix}$$

we find a bound for the inf–sup constant in terms of the smallest singular value $\lambda_{\min}$ of C, i.e.

$$\sup_{v^h \in \mathscr{V}^h} \frac{\int_\Gamma \mu^h [v^h] \mathrm{d}\Gamma}{\|v^h\|_{1;\Omega}} \geqslant c \inf_{w \in \mathbb{R}^{2n-1}} \frac{\|Cw\|}{\|w\|} \|\mu^h\|_{\sqrt{h};\Gamma} = \frac{1}{\|C^{-1}\|} \|\mu^h\|_{\sqrt{h};\Gamma}$$

where $\|\cdot\|$ denotes the Euclidean vector norm. A simple straightforward computation yields $\lambda_{\min} = \mathcal{O}(h)$. □

Remark 3.2
The second counterexample also shows that the estimate in Lemma 3.1 is sharp and cannot be improved.

Remark 3.3
As it will be shown in the next sections, taking every second intersection node as degree of freedom for the discrete Lagrange multiplier space will result in a uniform inf–sup condition.

4. ALGORITHM TO DEFINE THE MESH ON THE INTERFACE

The interface Γ is cutting through edges of the two-dimensional mesh $\mathscr{T}_h$ defining a graph. The vertices of this graph are vertices of the mesh $\mathscr{T}_h$, which are located exactly on Γ or are intersection nodes of an open edge of the mesh $\mathscr{T}_h$ and Γ. Once all the vertices of the graph have been marked, we connect the vertices based on the following rule: two vertices are connected in the graph if both of them result from the intersection of an open edge with Γ and the associated two edges share an endpoint. We note that vertices being vertices of the original mesh are always isolated vertices. In Figure 3, Γ is indicated by a dashed line. On the left, the mesh is aligned with the interface and the graph is a set of isolated vertices. On the right, the interface crosses elements, but the vertices are not connected because they do not lie on edges sharing common nodes. The situation is different in Figure 4, here vertices of the graph are connected.

The naive approach for building the Lagrange multiplier space is to set one independent multiplier on each vertex of the graph. We know that this does not pass the numerical inf–sup test [19], and as we have shown in the previous section counterexamples can be found.

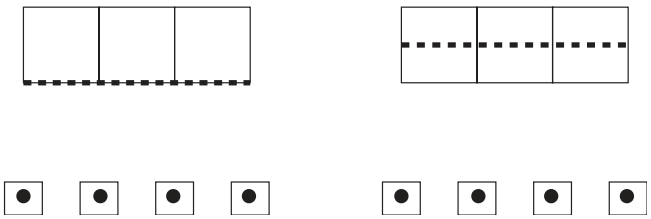

Figure 3. A mesh conforming to Γ (left) and not conforming (right). Below each case is the vertex graph as well as the selected vital vertices (squared).

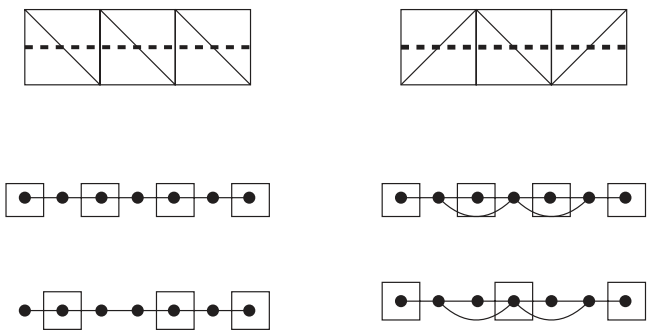

Figure 4. Two different situations of a non-adapted mesh. Below each case is the vertex graph as well as possible vital vertices.

We thus choose to select a subset of the vertices in the graph to define independent Lagrange multipliers. We call them vital vertices. They are selected based on the following rules:

(i) An isolated vertex is always vital.
(ii) A vital vertex is not allowed to be connected to any other vital vertex.
(iii) A non-vital vertex must be connected to at least one vital vertex.

The squared vertices in Figures 3 and 4 are vital. Note that for a given graph, the choice of vital vertices is not unique, see Figure 4.

The algorithm for the selection of the vital vertices that is used in the implementation closely follows the rules defined above. It can handle 3D problems with surface boundary conditions as well.

Algorithm in two dimensions and three dimensions used to define the vital vertices

0. Define an empty set of vital vertices called $vital$ and an empty set of regular (non-vital) vertices called non_vital.
1. The vertices on the interface that are also vertices of the mesh are introduced in the vital set. The rest of the vertices on the interface, denoted by V, emanate from cut edges. For each such vertex $v_i \in V$, we denote by $v_i[k], k=0,1,\ldots,$ the end-points of the cutting edge.
2. For every vertex $v_i \in V$ on the interface, count the number of intersections of the interface by the edges incident to $v_i[k]$. This defines the set $n_{\text{int}}[v_i]$.

3. Sort the set $n_{\text{int}}[v_i]$ (low number of intersections first).
4. Loop: Pick up the first item of $n_{\text{int}}[v_i]$ and the corresponding v_i.
5. Check that for the every node $v_i[k]$, none of its incident edges are intersecting the interface at an already vital vertex. If this condition is fulfilled, mark v_i as $vital$ and also mark every vertex that is the intersection of the interface from an edge incident to $v_i[k]$ as non_vital. If the condition does not hold, simply mark v_i as non_vital.
6. Remove v_i from $n_{\text{int}}[v_i]$.
7. If $n_{\text{int}}[v_i]$ is not empty, go to 4.
8. The set called $vital$ contains the vital vertices. The set called non_vital contains the other vertices.

The algorithm above is defined in such a way that isolated vertices (vertices on the interface that are also part of the mesh) are handled first and thus always declared as vital vertices. For other vertices of the interface, the classification should ensure a deterministic list of vital vertices. However, there are many (to a combinatorial extent) acceptable sets of vital vertices. Now, the vital vertices define the one-dimensional mesh on Γ which is used for the construction of the Lagrange multiplier space. More precisely, we associate one degree of freedom with each vital vertex, and the support of the associated nodal basis function is exactly the two adjacent one-dimensional elements. The shape function corresponding to this degree of freedom is the trace of a sum of related shape functions from the domain. For an isolated vital vertice, the shape function is the trace of the shape function of the node coming from the domain's mesh. We shall define exactly the shape functions in the sequel. Each element e of the one-dimensional mesh $\mathscr{E}_h$ has vital vertices as endpoints and is given as the union of straight segments joining two vertices of the graph. The length of the element is then given as the sum of the length of the straight subsegments. To find all elements $e \in \mathscr{E}_h$, we start from one vital vertex and follow the straight segments until the next vital vertex is reached, see Figure 5.

Remark 4.1
Roughly speaking criterion (iii) makes the set of vital vertices as large as possible to get a good best approximation property for the discrete Lagrange multiplier space, and criterion (ii) makes the dimension of $\mathscr{L}^h$ as small as necessary to satisfy a uniform inf–sup condition. Criterion (i) guarantees that in the case of an aligned interface, the one-dimensional mesh is inherited from the two-dimensional mesh.

The set of vital vertices on Γ is denoted by $\mathscr{V}_h$, and the dimension of the discrete Lagrange multiplier space $\mathscr{L}^h$ will be equal to $\#\mathscr{V}_h$. We point out that $\mathscr{V}_h \cap \mathscr{P}_h$ can be the empty set, where $\mathscr{P}_h$ is the set of all vertices of the two-dimensional mesh not on $\bar{\Gamma}_{\text{D}}$.

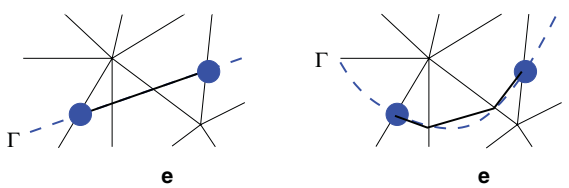

Figure 5. Element decomposed into three subsegments of the one-dimensional mesh for a straight (left) and curved (right) interface.

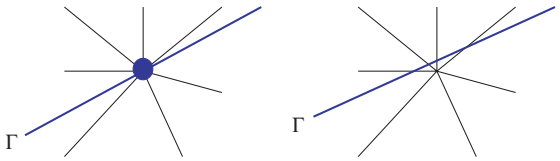

Figure 6. A vital vertex $p \in \mathscr{P}_h$ (left) and a small perturbation of Γ (right).

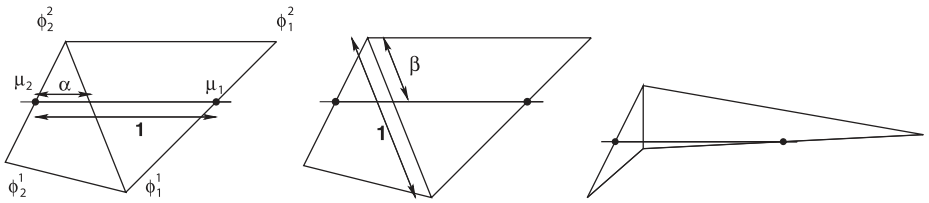

Figure 7. Decomposition of a scaled element in $\mathscr{E}_h$ into two subsegments by the underlying mesh: regular situation (left, middle) and an irregular case (right).

Figure 6 illustrates the influence of a small perturbation. On the left, the intersection of Γ with the mesh $\mathscr{T}_h$ has locally one cut which is a vertex in $\mathscr{P}_h$ and by criterion (i) it is a vital vertex. The situation is totally different if a small perturbation on Γ is imposed. On the right, we observe now four intersection nodes. Owing to criterion (iii) at least one of them has to be vital and due to criterion (ii) at most one of them can be vital. Thus, exactly one of the four intersection nodes will be vital, and the dimension of $\mathscr{L}^h$ does not change under a small perturbation.

5. DEFINITION OF A STABLE LAGRANGE MULTIPLIER SPACE

Starting with the one-dimensional mesh constructed in the previous section, we introduce in this section a new Lagrange multiplier space. One natural possibility is to use standard hat functions associated with the one-dimensional mesh on Γ as in [21]. More precisely, for each vital vertex the piecewise linear and continuous hat function is taken as the basis function. As a result, the Lagrange multiplier space does not see the underlying two-dimensional mesh. Thus, we do not follow this line but define the Lagrange multiplier basis functions as a trace of standard finite elements. This choice is motivated by the observation that in the inf–sup condition an element of $\mathscr{L}^h$ meets the trace of an element in $\mathscr{W}^h$. Moreover, this approach easily carries over to curved interfaces and to three dimensions, whereas a definition of the Lagrange multipliers based on a surface mesh induces complications.

Before we give the definition of our new Lagrange multiplier space, we consider locally the difference between the two construction principles. Figure 7 shows the influence of the underlying two-dimensional mesh. The two endpoints of an element of the one-dimensional mesh $\mathscr{E}_h$ on Γ are marked with filled bullets and are by construction vital vertices. We recall that in the case that Γ is not a straight line, the elements of $\mathscr{E}_h$ do not have to be straight segments.

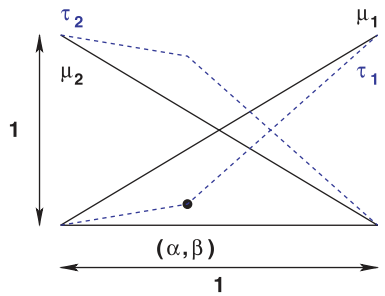

Figure 8. Local trace of a finite element and standard hat function.

By μ_1 and μ_2, we denote the two nodal local hat functions on a scaled element of $\mathscr{E}_h$ of length one, and we set τ_i, $i=1,2$, as the trace of $\phi_i^1+\phi_i^2$. The two sets of functions $\{\mu_1,\mu_2\}$ and $\{\tau_1,\tau_2\}$ are shown in Figure 8. In contrast to μ_i, τ_i is only piecewise linear on the one-dimensional element.

A straightforward computation gives for $N:=(n_{ij})_{1\leqslant i,j\leqslant 2}$, $M:=(m_{ij})_{1\leqslant i,j\leqslant 2}$, with $n_{ij}=\int_0^1 \tau_i\mu_j\,\mathrm{d}s$, $m_{ij}=\int_0^1 \tau_i\tau_j\,\mathrm{d}s$

$$N=\begin{pmatrix} b_n & a_n-b_n \\ 0.5-b_n & 0.5+b_n-a_n \end{pmatrix},\quad M=\begin{pmatrix} b_m & a_m-b_m \\ a_m-b_m & 1-2a_m+b_m \end{pmatrix}$$

where $a_n:=\int_0^1 \tau_1\,\mathrm{d}s$, $b_n:=\int_0^1 \tau_1\mu_1\,\mathrm{d}s$, $a_m=a_n$ and $b_m:=\int_0^1 \tau_1\tau_1\,\mathrm{d}s$. We note that both pairs $\{\mu_1,\mu_2\}$ and $\{\tau_1,\tau_2\}$ form a positive partition of unity, i.e. $\tau_1+\tau_2=1=\mu_1+\mu_2$ and $\mu_i,\tau_i\geqslant 0$. It is obvious that the mass matrix M is symmetric and positive definite. Moreover, there exists a constant depending only on the shape regularity of the two-dimensional mesh such that $x^\top Mx\geqslant c\|x\|^2$. For the non-symmetric matrix N, the situation is different. Although the eigenvalues of N are positive, we find that for some cases of $(\alpha,\beta)\in(0,1)^2$ the matrix is not positive, i.e. there exits a x such that $x^\top Nx<0$. These cases are called irregular, the other ones regular. We consider now N in more detail, and find for $x^\top=(x_1,x_2)$

$$x^\top Nx=b_nx_1^2+(\tfrac{1}{2}+a_n-2b_n)x_1x_2+(\tfrac{1}{2}+b_n-a_n)x_2^2$$

It is easy to see that $0.5>b_n>0$ and $b_n<a_n<b_n+0.5$. To verify if N is positive, we have to consider the sign of the minimum of a quadratic expression given by

$$b_n-\frac{(\frac{1}{2}-2b_n+a_n)^2}{2+4b_n-4a_n}$$

Equivalently, we have to ask for the sign of $4b_n-(a_n+0.5)^2$. Using $a_n=0.5(1+\beta-\alpha)$ and $b_n=(2+(\beta-\alpha)(1+\alpha))/6$, we find that N is positive if

$$(1+\tfrac{1}{2}(\beta-\alpha))^2<\tfrac{2}{3}(2+(\beta-\alpha)(1+\alpha))$$

A straightforward computation shows that for

$$\beta\gtrless\alpha+\tfrac{2}{3}((2\alpha-1)\pm\sqrt{(2\alpha-1)^2+3})$$

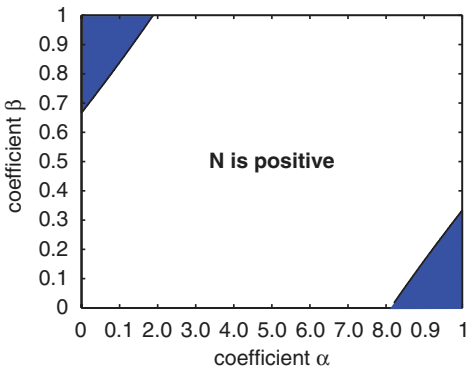

Figure 9. Subdomain where N is positive.

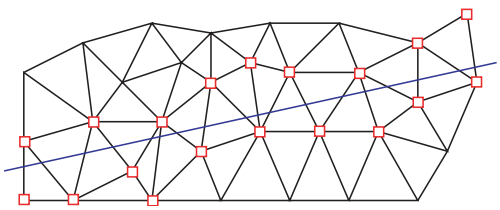

Figure 10. Set of vertices in $\mathscr{P}_h^\Gamma$.

the matrix N is not positive, see also Figure 9. If (α, β) is placed in the shadowed region, we have a irregular case in which we cannot expect to obtain locally per element a inf–sup condition, and thus it is extremely difficult to analyze the general case of unstructured meshes.

This simple local computation motivates our choice not to take as Lagrange multiplier a linear function on the one-dimensional elements of the interface mesh but a trace. In that case, the proof of a uniform inf–sup can be realized locally.

For each vital vertex $p \in \mathscr{V}_h$, we define the associated basis function $\mu_p \in \mathscr{L}^h$ as a linear combination of some nodal hat functions $\phi_q, q \in \mathscr{P}_h$ restricted to Γ. The definition of the coefficients is based on some preliminary observations and remarks. We note that the number of vertices in $\mathscr{P}_h$ such that $\phi_q|_\Gamma$ is not equal to zero is of order h^{-1}. Introducing the subset $\mathscr{P}_h^\Gamma$, see Figure 10, by

$$\mathscr{P}_h^\Gamma := \{p \in \mathscr{P}_h; \phi_p|_\Gamma \text{ not identical zero}\}$$

it is trivial to see that $\sum_{q\in\mathscr{P}_h} \alpha_{pq}\phi_q|_\Gamma = \sum_{q\in\mathscr{P}_h^\Gamma} \alpha_{pq}\phi_q|_\Gamma$, and thus we set

$$\mu_p := \sum_{q\in\mathscr{P}_h^\Gamma} \alpha_{pq}\phi_q|_\Gamma, \quad p \in \mathscr{V}_h \tag{14}$$

In a next step, we define for each vital vertex $q \in \mathscr{V}_h$ a $\mathscr{P}_q \subset \mathscr{P}_h^\Gamma$. We recall that each vital vertex q is in $\mathscr{P}_h$ or is the intersection point of an open edge e_q of the mesh $\mathscr{T}_h$. In the first case, we set

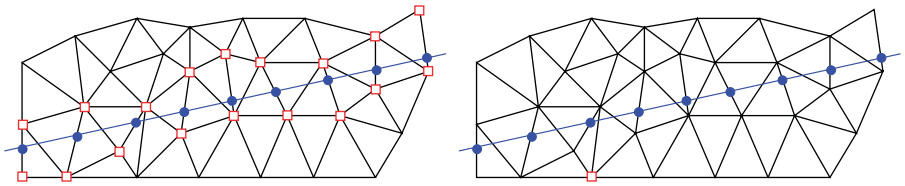

Figure 11. The set of vertices in $\mathscr{P}_h^{\mathscr{V}}$ (left) and in $\mathscr{Q}_h^{\Gamma}$ (right) are marked with empty squares, the vertices in $\mathscr{V}_h$ are marked with filled circles.

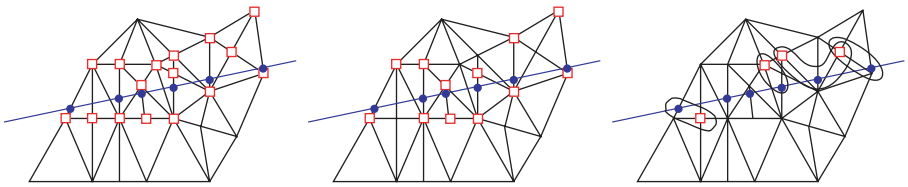

Figure 12. Sets of vertices from the left to the right $\mathscr{P}_h^{\Gamma}$, $\mathscr{P}_h^{\mathscr{V}}$, $\mathscr{Q}_h^{\Gamma}$ and Q_p.

$\mathscr{P}_q := \{q\}$ and in the second case, we define $\mathscr{P}_q := \{p_q^1, p_q^2\}$, where p_q^1, p_q^2 are the two endpoints of e_q. In addition, we set

$$\mathscr{Q}_h^{\Gamma} := \mathscr{P}_h^{\Gamma} \Big\backslash \bigcup_{q \in \mathscr{V}_h} \mathscr{P}_q =: \mathscr{P}_h^{\Gamma} \setminus \mathscr{P}_h^{\mathscr{V}}$$

and observe that $\mathscr{Q}_h^{\Gamma}$ might be the empty set. Owing to Criterion (iii), each $q \in \mathscr{Q}_h^{\Gamma}$ is connected by at least one closed edge $\bar{e}_q$ cutting the interface with an element in $\mathscr{P}_h^{\mathscr{V}}$, see also Figure 11. The number of such edges e_q, i.e. one endpoint is q, the other endpoint q_o is in $\mathscr{P}_h^{\mathscr{V}}$ and $\bar{e}_q \cap \Gamma$ is not empty, is denoted by n_q. Because all $\mathscr{P}_p$, $p \in \mathscr{V}_h$, are pairwise disjoint, there exists a unique $p \in \mathscr{V}_h$ such that $q_o \in \mathscr{P}_p$, and we put q into $\mathscr{Q}_p$, i.e. $\bigcup_{p \in \mathscr{V}_h} \mathscr{Q}_p = \mathscr{Q}_h^{\Gamma}$.

In the example of the right picture in Figure 12, $n_q = 1$ or $n_q = 2$. We note that $\mathscr{Q}_p$ can be empty and that $\mathscr{Q}_p \cap \mathscr{Q}_q$ does not have to be empty for $p, q \in \mathscr{V}_h$, see the right picture in Figure 12.

In terms of these subsets, we define now the values of the coefficients α_{pq}, $p \in \mathscr{V}_h$, $q \in \mathscr{P}_h^{\Gamma}$

$$\alpha_{pq} := \begin{cases} 1, & q \in \mathscr{P}_p \\ \dfrac{1}{n_q}, & q \in \mathscr{Q}_p \\ 0 & \text{otherwise} \end{cases}$$

Then μ_p has a local support and can be written as

$$\mu_p = \sum_{q \in \mathscr{P}_p} \phi_q + \sum_{q \in \mathscr{Q}_p} \frac{1}{n_q} \phi_q \tag{15}$$

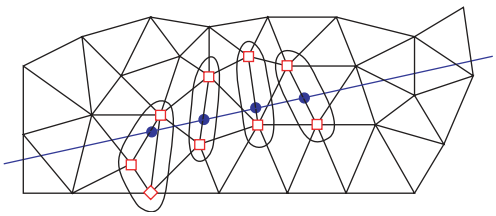

Figure 13. Nodes in $\mathscr{P}_p$ are marked with a square, nodes in $\mathscr{Q}_p$ with a diamond.

Figure 13 shows which nodes $q \in \mathscr{P}_h^\Gamma$ contribute to the definition of μ_p, $p \in \mathscr{V}_h$.

Lemma 5.1
The set $\{\mu_p\}_{p\in\mathscr{V}_h}$ forms a positive partition of unity with local supports on Γ, i.e.

$$\sum_{p\in\mathscr{V}_h} \mu_p = 1$$

Proof
Observing that the number of $p \in \mathscr{V}_h$ such that $q \in \mathscr{Q}_p$ is exactly n_q for $q \in \mathscr{Q}_h^\Gamma$, a straightforward computation shows that

$$\sum_{p\in\mathscr{V}_h} \mu_p = \sum_{p\in\mathscr{V}_h} \left(\sum_{q\in\mathscr{P}_p} \phi_q + \sum_{q\in\mathscr{Q}_p} \frac{1}{n_q}\phi_q \right) = \sum_{q\in\mathscr{P}_h^{\mathscr{V}}} \phi_q + \sum_{q\in\mathscr{Q}_h^\Gamma} \frac{1}{n_q}\phi_q \sum_{p\in\mathscr{V}_h, q\in\mathscr{Q}_p} 1$$
$$= \sum_{q\in\mathscr{P}_h^{\mathscr{V}}} \phi_q + \sum_{q\in\mathscr{Q}_h^\Gamma} \phi_q = \sum_{q\in\mathscr{P}_h^\Gamma} \phi_q = 1 \qquad \square$$

Remark 5.2
Lemma 5.1 yields that the Lagrange multiplier space $\mathscr{L}^h$ reproduces constants and thus the best approximation property gives an $\mathscr{O}(h)$ term in the *a priori* analysis.

Let $q \in \mathscr{Q}_h^\Gamma$ then there exists at least one $p \in \mathscr{V}_h$ such that $q \in \mathscr{Q}_p$, and thus $\mathscr{Q}^q := \{p \in \mathscr{V}_h,$ such that $q \in \mathscr{Q}_p\}$ is not empty. Then it is easy to see that under the condition

$$\sum_{p\in\mathscr{Q}^q} \alpha_{pq} = 1$$

Lemma 5.1 is still valid. This observation allows us to replace the trivial choice $\alpha_{pq} = 1/n_q$ by a more sophisticated one. A better choice for $\alpha_{pq} \geqslant 0$ takes into account the distances between q and all $p \in \mathscr{Q}^q$. The closer the q is to p, the larger the scaled coefficient should be.

In the rest of this section, we show that our newly constructed Lagrange multiplier space $\mathscr{L}^h$ satisfies a uniform inf–sup condition. We start with some preliminary results for the one-dimensional mesh on the interface defining $\mathscr{L}^h$. We recall that $\mathscr{E}_h$ is the set of elements of the one-dimensional mesh on Γ and note that each $e \in \mathscr{E}_h$ has as endpoints vital vertices.

Lemma 5.3
There exist constants independent of the mesh-size such that for all elements $e \in \mathscr{E}_h$

$$ch_T \leqslant h_e \leqslant Ch_T, \quad T \in \mathscr{T}_e \tag{16}$$

where h_e is the length of e, and h_T is the diameter of the element T, and $\mathscr{T}_e \subset \mathscr{T}_h$ is the set of all elements T such that the intersection with e is not empty.

Proof
By construction, criterion (ii) yields that the vital vertices cannot be too close together, and criterion (iii) guarantees that h_e is not too large.

As a result from the previous lemma, we find that the one-dimensional mesh for $\mathscr{L}^h$ is regular in the sense that

$$ch_e \leqslant h_{\hat{e}} \leqslant Ch_e$$

for all edges $e, \hat{e} \in \mathscr{E}_h$ with $\partial e \cap \partial \hat{e}$ is a vital vertex. □

Theorem 5.4
There exists a constant independent of the mesh-size such that for all $\mu^h \in \mathscr{L}^h$

$$\sup_{v^h \in \mathscr{U}^h} \frac{\int_\Gamma \mu^h [v^h] \, \mathrm{d}\Gamma}{\|v^h\|_{1;\Omega}} \geqslant c \|\mu^h\|_{-1/2;\Gamma_h}$$

Proof
By definition of $\mathscr{L}^h$, the basis functions are associated with the vital vertices and are given as the trace of a linear combination of standard hat functions. In terms of (15), each $\mu^h \in \mathscr{L}^h$ has the form $\mu^h = \sum_{p \in \mathscr{V}_h} \alpha_p \mu_p$. For simplicity, we assume that the mesh $\mathscr{E}_h$ is globally quasi-uniform on Γ. However, this is a technical assumption that is not necessary for the proof as a detailed analysis shows. Using the definition of the X-FEM space $\mathscr{U}^h$, we set $w^h = \sum_{p \in \mathscr{V}_h} \alpha_p (\sum_{q \in \mathscr{P}_p^1} \phi_q + \sum_{q \in \mathscr{Q}_p^1} (1/n_q) \phi_q) \chi_1 - \sum_{p \in \mathscr{V}_h} \alpha_p (\sum_{q \in \mathscr{P}_p^2} \phi_q + \sum_{q \in \mathscr{Q}_p^2} (1/n_q) \phi_q) \chi_2$, where χ_i is the Heaviside function with respect to Ω_i, $i = 1, 2$, $\mathscr{P}_p^1 := \{q \in \mathscr{P}_p, q \in \bar{\Omega}_1\}$, $\mathscr{Q}_p^1 := \{q \in \mathscr{Q}_p, q \in \bar{\Omega}_1\}$, $\mathscr{P}_p^2 := \mathscr{P}_p \setminus \mathscr{P}_p^1$, $\mathscr{Q}_p^2 := \mathscr{Q}_p \setminus \mathscr{Q}_p^1$. The definition of w^h yields $\mu^h = [w^h]_{|\Gamma}$ and thus $\int_\Gamma \mu^h [w^h] \, \mathrm{d}\Gamma = \|\mu^h\|_{-1/2;\Gamma_h} \|[w^h]\|_{1/2;\Gamma_h}$. Owing to the construction of w^h and Lemma 5.3, it is easy to see that $\|[w^h]\|_{1/2;\Gamma_h}^2$ is equivalent to $\sum_{p \in \mathscr{V}_h} \alpha_p^2$. Then a standard inverse estimate for finite elements yields $\|w^h\|_{1;\Omega}^2 \leqslant C \sum_{p \in \mathscr{V}_h} \alpha_p^2$ and thus

$$\sup_{v^h \in \mathscr{U}^h} \frac{\int_\Gamma \mu^h [v^h] \, \mathrm{d}\Gamma}{\|v^h\|_{1;\Omega}} \geqslant \frac{\int_\Gamma \mu^h [w^h] \, \mathrm{d}\Gamma}{\|w^h\|_{1;\Omega}} = \|\mu^h\|_{-1/2;\Gamma_h} \frac{\|[w^h]\|_{1/2;\Gamma_h}}{\|w^h\|_{1;\Omega}} \geqslant c \|\mu^h\|_{-1/2;\Gamma_h}$$

As a consequence of Theorem 5.4 and Lemmas 5.3 and 5.1, we find that the discrete saddle-point formulation (4)–(5) is stable and optimal *a priori* estimates holds. □

Remark 5.5
Both algorithms, the one to construct the vital vertices and the one to define the basis functions of $\mathscr{L}^h$ are not restricted to the two-dimensional setting. They can easily be generalized to the

three-dimensional case. Using the alternative approach of using standard hat functions for the Lagrange multiplier on the mesh $\mathscr{E}_h$ would require in three-dimensional to construct a mesh of the interface from the vital vertices that satisfies some regularity requirements (e.g. using a Delaunay approach). By using for the definition of the Lagrange multiplier shape functions defined on the background mesh this can be avoided.

6. NUMERICAL RESULTS

In this section, we show some numerical results illustrating the influence of the inf–sup condition on the error decay. Different Lagrange multiplier spaces are compared and tested on unstructured meshes with different mesh-sizes.

A comparison is made between different Lagrange multiplier spaces including:

- The naïve Lagrange multiplier space.
- Lagrange multipliers on a boundary-fitted mesh.
- The Lagrange multiplier space found in [21].
- Our newly constructed Lagrange multiplier space.

6.1. Dirichlet boundary condition

We consider a two-dimensional Laplace model problem already considered in [12, 21]. The problem is defined over the unit-square $\Omega := \Omega_1 := (0,1)^2$, and the exact solution is given by

$$u(x,y) = [\cosh(\pi y) - \coth(\pi)\sinh(\pi y)]\sin(\pi x) \tag{17}$$

see Figure 14. The boundary conditions and the right-hand side are selected according to (17), where $\Gamma := \Gamma_D := \{(s,0), 0<s<1\}$ and $1/k = 0$, $\Gamma_N := \partial\Omega \setminus \bar{\Gamma}$.

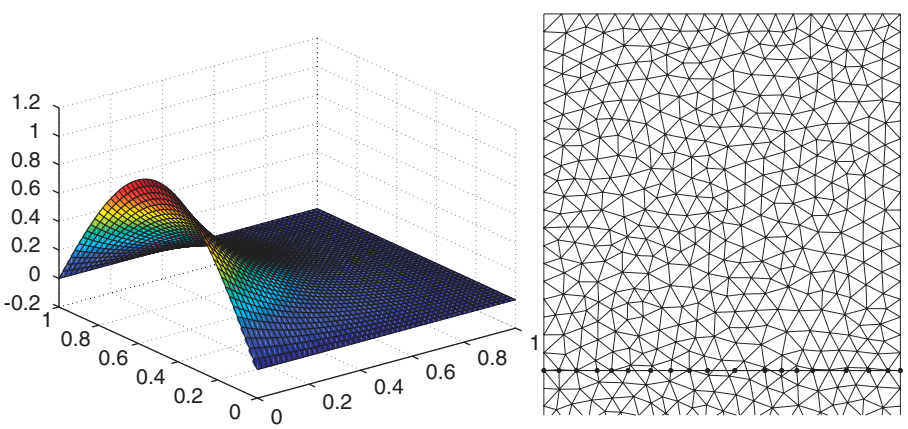

Figure 14. The exact solution of the two-dimensional Laplace model problem (left) and a non-matching mesh $h = \frac{1}{20}$ (right). The boundary Γ is given by the horizontal line at the bottom and the vital vertices are marked by filled bullets.

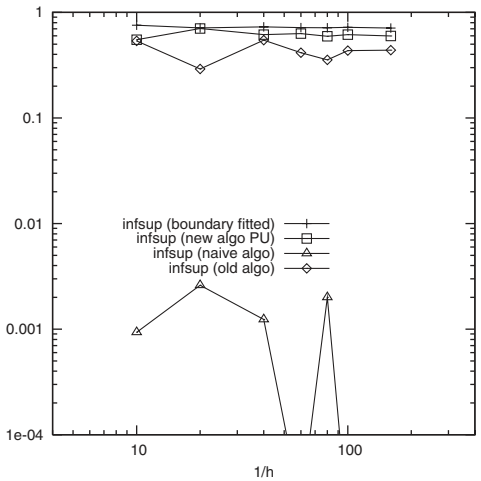

Figure 15. Numerical computed inf–sup value.

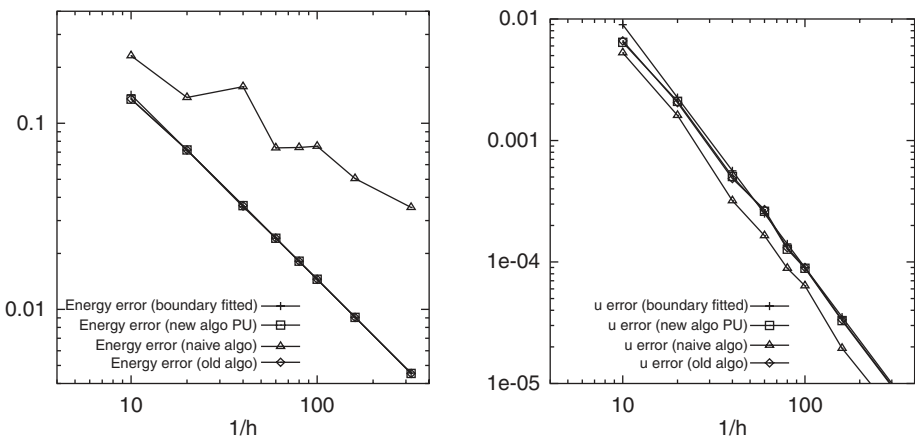

Figure 16. Discretization error in the energy norm and on the Dirichlet boundary.

Figure 15 shows the numerical computed inf–sup constant on different meshes. It is obvious that the naive approach does not yield a uniform inf–sup estimate, whereas the other approaches satisfy a uniform inf–sup condition.

As a result, for the naive approach, the error in the energy norm does not decay optimally, see Figure 16. The other choices provide the same qualitative and almost the same quantitative results for the error in the energy norm and the error on the Dirichlet boundary condition.

The new Lagrange multiplier has a smaller error in the Lagrange multiplier and a better inf–sup constant. However, this difference is not significant, see Figures 15 and 17.

The main advantage of the newly designed approach is its stability in combination with its simple local selection process of vital vertices.

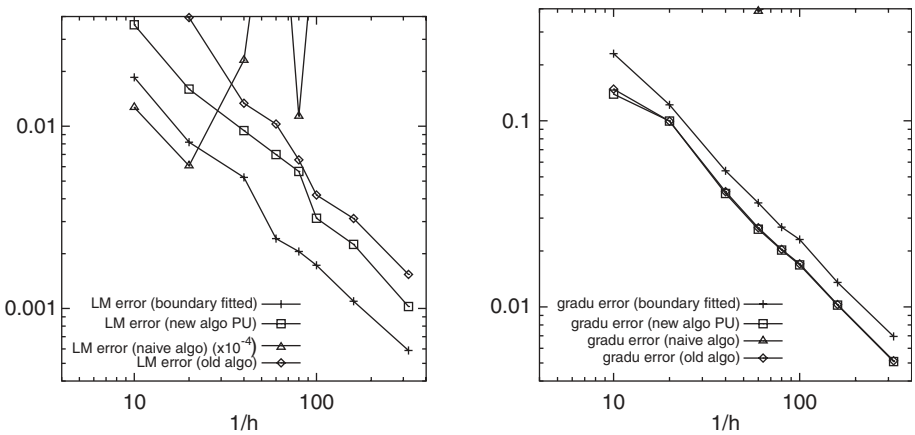

Figure 17. Error of the Lagrange multiplier (left) and of the gradient (right) on Γ.

6.2. Interface between two materials

Here, we model an interface between two domains with different mechanical properties. The material law is linear isotropic elasticity. The outer domain is the matrix and has the following mechanical properties: $E_{\mathrm{m}}=1.0$ and $\nu_{\mathrm{m}}=0.3$. It has a circular shape; its radius is $r_{\mathrm{m}}=2$. The inclusion is contained inside the matrix and is also circular; its radius is $r_i=0.4$. It has the following mechanical properties: $E_i=10$ and $\nu_i=0.25$. We have done computations in a two-dimensional setting with the assumptions of plane strain and that both domains are perfectly bonded together unless otherwise stated. As sole boundary condition, at the radius $r=r_{\mathrm{m}}$, a uniform tension is applied so that the radial displacement $u_r|_{r=r_{\mathrm{m}}}$ is equal to r_{m}. The discretization consists of separate displacement fields for each domain, bound together via the Lagrange multiplier space described in this article. The weak form corresponds to Equations (2) and (3), with remarks made in the sequel of those equations. For a perfectly bonded interface, the term including the $1/k$ factor vanishes; but if an interfacial finite stiffness exists then this term has to be taken into account and eventually produces jumps in the primal variable (see Figure 20).

The exact solution for the perfectly bonded interface is as follows [9]:

$$u(r,\theta)=\begin{cases}\left[\left(1-\dfrac{b^2}{a^2}\right)\alpha+\dfrac{b^2}{a^2}\right]r & \text{for } r<a\\[2ex] \left(r-\dfrac{b^2}{r}\right)\alpha+\dfrac{b^2}{r} & \text{for } a\leqslant r\leqslant b\end{cases} \tag{18}$$

where

$$\alpha=\frac{(\lambda_i+\mu_i+\mu_m)b^2}{(\lambda_m+\mu_m)a^2+(\lambda_i+\mu_i)(a^2+b^2)+\mu_m b^2}$$

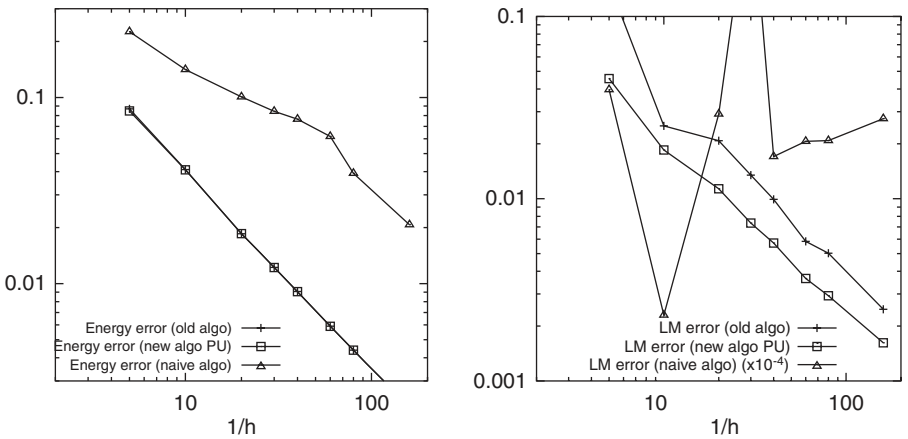

Figure 18. Error in the energy norm (left) and on the Lagrange multiplier (right) for the interface problem.

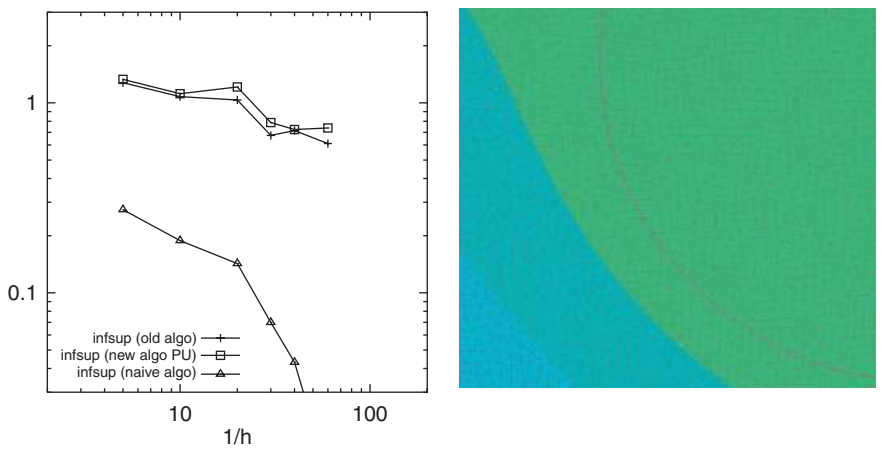

Figure 19. Inf–sup value (left) and zoom on the interface (right).

Here, λ_i, μ_i, λ_m and μ_m are the Lamé constants:

$$\lambda = \frac{vE}{(1+v)(1-2v)}$$

$$\mu = \frac{E}{2(1+v)}$$

Knowing $u(r,\theta)$, the strain and stresses are obtained by simple differentiation. Thus, the error in energy norm and the error on the Lagrange multipliers may be obtained without difficulty (Figures 18–20).

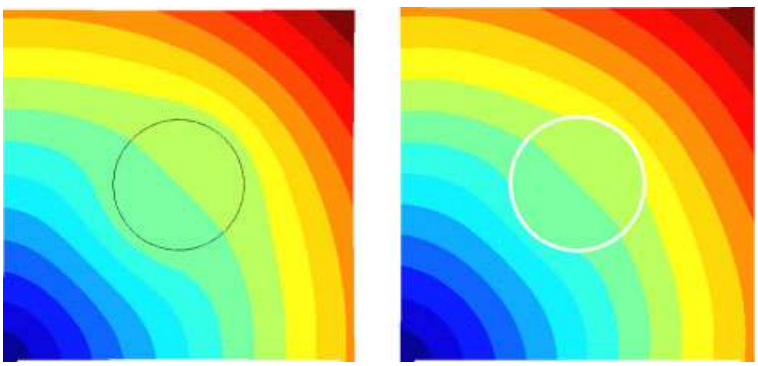

Figure 20. Displacements for a perfectly bonded interface (left) and a slightly compliant interface (right) . Please note the gap (jump in the displacements).

As for the example in Section 6.1, the new Lagrange multiplier space behaves properly and is numerically stable.

7. CONCLUSIONS

In this paper we did introduce a new way to build a Lagrange multiplier space to enforce stiff boundary condition in the extended finite element method, i.e. along boundaries not matching the mesh. The originality of the new space is that it is the trace of the classical inner space on the boundary with appropriate linear combination between the inner nodes. It is proven mathematically that the new space passes the LBB condition for two-dimensional problems.

REFERENCES

1. Babuška I, Melenk I. Partition of unity method. *International Journal for Numerical Methods in Engineering* 1997; **40**(4):727–758.
2. Melenk JM, Babuška I. The partition of unity finite element method: basic theory and applications. *Computer Methods in Applied Mechanics and Engineering* 1996; **39**:289–314.
3. Belytschko T, Black T. Elastic crack growth in finite elements with minimal remeshing. *International Journal for Numerical Methods in Engineering* 1999; **45**(5):601–620.
4. Moës N, Dolbow J, Belytschko T. A finite element method for crack growth without remeshing. *International Journal for Numerical Methods in Engineering* 1999; **46**:131–150.
5. Sukumar N, Moës N, Belytschko T, Moran B. Extended finite element method for three-dimensional crack modelling. *International Journal for Numerical Methods in Engineering* 2000; **48**(11):1549–1570.
6. Moës N, Gravouil A, Belytschko T. Non-planar 3D crack growth by the extended finite element and level sets. Part I: mechanical model. *International Journal for Numerical Methods in Engineering* 2002; **53**:2549–2568.
7. Belytschko T, Moës N, Usui S, Parimi C. Arbitrary discontinuities in finite elements. *International Journal for Numerical Methods in Engineering* 2001; **50**:993–1013.
8. Daux C, Moës N, Dolbow J, Sukumar N, Belytschko T. Arbitrary branched and intersecting cracks with the extended finite element method. *International Journal for Numerical Methods in Engineering* 2000; **48**:1741–1760.
9. Sukumar N, Chopp DL, Moës N, Belytschko T. Modeling holes and inclusions by level sets in the extended finite element method. *Computer Methods in Applied Mechanics and Engineering* 2001; **190**:6183–6200.
10. Moës N, Cloirec M, Cartraud P, Remacle J-F. A computational approach to handle complex microstructure geometries. *Computer Methods in Applied Mechanics and Engineering* 2003; **192**:3163–3177.

11. Nitsche J. Über ein Variationsprinzip zur Lösung von Dirichlet-Problemen bei Vervendung von Teilräumen, die keinen Randbedingungen unterworfen sind. *Abhandlungen aus dem Mathematischen Seminaren des Universität Hamburg* 1971; **36**:9–15.
12. Fernández-Méndez S, Huerta A. Imposing essential boundary conditions in mesh-free methods. *Computer Methods in Applied Mechanics and Engineering* 2004; **193**:1257–1275.
13. Hansbo A, Hansbo P. An unfitted finite element method, based on Nitsche's method, for elliptic interface problems. *Computer Methods in Applied Mechanics and Engineering* 2002; **191**:5537–5552.
14. Wriggers P, Zavarise G. A formulation for frictionless contact problems using a weak formulation introduced by Nitsche. *Computational Mechanics* 2008; **41**(3):407–420.
15. Mourad HM, Dolbow J, Harari I. A bubble-stabilized finite element method for Dirichlet constraints on embedded interfaces. *International Journal for Numerical Methods in Engineering* 2007; **69**(4):772–793.
16. Dolbow JE, Franca LP. Residual-free bubbles for embedded Dirichlet problems. *Computer Methods in Applied Mechanics and Engineering* 2008; **197**:3751–3759.
17. Stenberg R. On some techniques for approximating boundary conditions in the finite element method. *Journal of Computational and Applied Mathematics* 1995; **63**:139–148.
18. Dolbow J, Moës N, Belytschko T. An extended finite element method for modeling crack growth with frictional contact. *Computer Methods in Applied Mechanics and Engineering* 2001; **190**:6825–6846.
19. Ji H, Dolbow JE. On strategies for enforcing interfacial constraints and evaluating jump conditions with the extended finite element method. *International Journal for Numerical Methods in Engineering* 2004; **61**:2508–2535.
20. Simone A. Partition of unity-based discontinuous elements for interface phenomena: computational issues. *Communications in Numerical Methods in Engineering* 2004; **20**:465–478.
21. Moës N, Béchet E, Tourbier M. Imposing essential boundary conditions in the extended finite element method. *International Journal for Numerical Methods in Engineering* 2006; **67**:1641–1669.
22. Chapelle D, Bathe KJ. The inf–sup test. *Computers and Structures* 1993; **47**:537–545.
23. El-Abbasi N, Bathe KJ. Stability and patch test performance of contact discretizations and a new algorithm. *Computers and Structures* 2001; **79**:1473–1486.
24. Géniaut S, Massin P, Moës N. A stable 3D contact formulation for cracks using x-fem. *Revue Européenne de Mécanique Numérique* 2007; **16**:259–276.
25. Nistor I, Guiton MLE, Massin P, Moës N, Géniaut S. An X-FEM approach for large sliding contact along discontinuities. *International Journal for Numerical Methods in Engineering* 2008; accepted.
26. Kim TY, Dolbow J, Laursen T. A mortared finite element method for frictional contact on arbitrary interfaces. *Computational Mechanics* 2007; **39**(3):223–235.
27. Haslinger J, Renard Y. A new fictitious domain approach inspired by the extended finite element method. *SIAM Journal on Numerical Analysis* 2008; under review.
28. Babuška I. The finite element method with Lagrangian multipliers. *Numerische Mathematik* 1973; **20**:179–192.
29. Barbosa H, Hughes T. Finite element method with Lagrange multipliers on the boundary: circumventing the Babuska–Brezzi condition. *Computer Methods in Applied Mechanics and Engineering* 1991; **85**(1):109–128.
30. Brezzi F, Fortin M. *Mixed and Hybrid Finite Element Methods*. Springer Series in Computational Mathematics. Springer: Berlin, 1991.